Table XIX. Typical Dry Basis Composition of Zeolites Used in This Work (wt %)

zeolite	composition (wt %)				
	SiO_2	Al_2O_3	Na_2O	K_2O	CaO
KA (3A)	38.98	33.08	5.02	22.92	–
NaA (4A)	42.30	35.89	21.81	–	–
CaA (5A)	44.76	36.46	5.54	–	15.04
HAB A40	42.31	35.90	21.79	–	–
NaX (13X)	47.46	32.68	19.86	–	–
NaY	64.03	22.37	13.60	–	–
ZF520	95.87	4.07	0.06	–	–

dures to the synthesis of fine chemicals. In fact, many of the target molecules to be prepared in multistage syntheses are too bulky to be built in or to desorb from the zeolite pore systems, as the presently available structures peak at about 10-Å pore dimension.[66] Secondly, the properties of the NaX zeolite as a free-radical initiator for chlorinations in like and as efficient manner as benzoyl peroxide brings in a new dimension. It complements their common use as acidic catalysts. This is due to a useful attractive structural feature, the presence of oxy radical centers O_3M-O· (M = Al or Si) on the outer surface. Other aluminosilicates such as clays are known to have a wealth of such centers on their surface. A number of authors have drawn attention to them,[67-69] in particular Friedemann Freund in a very recent study.[67] The density of such centers is controllable to some extent; it can be increased by dehydrative activation of the surface alanol and silanol groups. Contact with these centers of aromatic molecules leads to radicals and to radical cations.[68,69] We had taken advantage of their presence already for designing effective aromatic nitrations[70] and for catalysis of the radical-cation mediated Diels–Alder reaction.[71] This new success at catalysis of aromatic chlorination is another illustration of the promise for chemistry inherent in these metal–oxy radical centers on the surface of inorganic solids. It has not escaped our attention that other chemical processes present a dichotomy between an ionic and a radical pathway, leading to different products or to differing product distributions. We plan to explore the potential of zeolite catalysts, such as the ZF520 and the NaX, respectively, to channel such reactions into one or the other of the two coexisting routes. Yet more generally, preparative organic chemistry in academic laboratories has much to gain from borrowing zeolites from their industrial birthplace.

Acknowledgment. We thank the Ecole Polytechnique for award of a fellowship to one of us (L.D.) and Professors Jacques Fraissard, Université Pierre-et-Marie Curie, Arthur Greenberg, New Jersey Institute of Technology, and Gary A. Eiceman, New Mexico State University, Las Cruces, for useful information. We thank the companies Degussa, Hanau, W. Germany, and Zeocat, Montoir de Bretagne, France, for samples of zeolites.

(66) Schwochow, F.; Puppe, L. *Angew. Chem., Int. Ed. Engl.* **1975**, *14*, 620–628.
(67) Freund, F.; Battlo, F.; Freund, M. *ACS Symp. Ser.* **1989**, *415*, 310–329.
(68) (a) Doner, H. E.; Mortland, M. M. *Science* **1969**, *166*, 1406–1407. (b) Pinnavaia, T. J.; Mortland, M. M. *J. Phys. Chem.* **1971**, *75*, 3957–3965. (c) Rupert, J. P. *J. Phys. Chem.* **1973**, *77*, 784–790. (d) Fenn, D.; Mortland, M. M.; Pinnavaia, T. J. *Clays Clay Miner.* **1973**, *21*, 315–322. (e) Pinnavaia, T. J.; Hall, P. L.; Cady, S. S.; Mortland, M. M. *J. Phys. Chem.* **1974**, *78*, 994–999.
(69) Bauld, N. L.; Bellville, D. J.; Harrirchian, B.; Lorentz, K. L.; Pabon, R. A.; Reynolds, D. W.; Wirth, D. D.; Chiou, H. S.; Marsh, B. K. *Acc. Chem. Res.* **1987**, *20*, 371–378.
(70) Cornélis, A.; Laszlo, P.; Pennetreau, P. *Bull. Soc. Chim. Belg.* **1984**, *93*, 961–971.
(71) Laszlo, P.; Moison, H. *Chem. Lett.* **1989**, 1031–1034.

Norrish Type I and Type II Reactions of Ketones as Photochemical Probes of the Interior of Zeolites[†,‡]

V. Ramamurthy,* D. R. Corbin, and D. F. Eaton

Central Research and Development Department, E. I. du Pont de Nemours and Company, Experimental Station, P.O. Box 80 328, Wilmington, Delaware 19880-0328

Received March 13, 1990

The Norrish type I and type II reactions of alkylbenzoin ethers, alkyldeoxybenzoins and α-alkyldibenzyl ketones included within the microporous structures of zeolites X and Y have been investigated. Product distributions varied significantly from that observed in benzene. In addition, it differed between various alkali-metal cation-exchanged samples. These variations are interpreted to result from the restriction offered by the zeolite micropores on the motions of the adsorbed organic molecule. Although this study is restricted to ketones, the knowledge gained is expected to be of general value.

Introduction

Photochemical and photophysical properties of organic molecules are considerably altered when they become part of an organized or constrained structure.[1] In this context, the internal structure (pores and cages) of zeolites have attracted recent attention.[2-4] This paper presents a study

[†] Part of the series on Modification of Photochemical Reactivity by Zeolites. For other members of the series, see ref 4.
[‡] Contribution no. 5419.

(1) Ramamurthy, V. *Tetrahedron* **1986**, *42*, 5753 and references therein. Ramamurthy, V.; Scheffer, J. R.; Turro, N. J. *Tetrahedron* **1987**, *43*, 1197–1745. Kalayanasundaram, K. *Photochemistry in Microheterogeneous Systems*; Academic: New York, 1987. Weiss, R. G. *Tetrahedron* **1988**, *44*, 3413. Scheffer, J. R.; Trotter, J. *Rev. Chem. Int.* **1988**, *9*, 271. Fox, M. A. *Top. Curr. Chem.* **1987**, *142*, 71. Anpo, M.; Matsuura, T. *Photochemistry on Solid Surfaces*; Elsevier: Amsterdam, 1989.

0022-3263/90/1955-5269$02.50/0

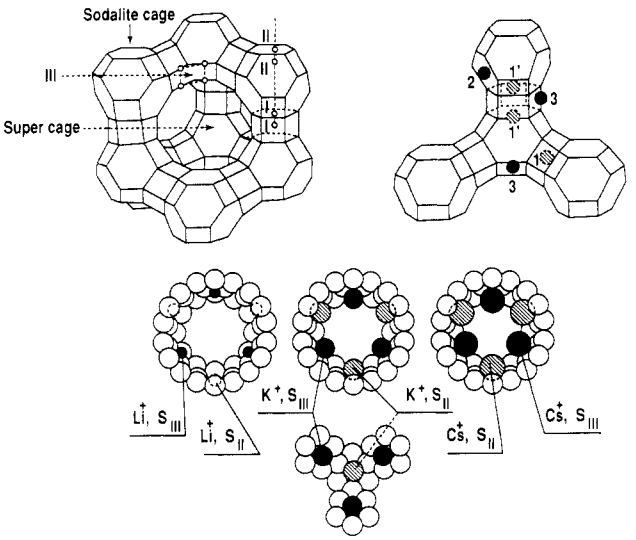

Figure 1. Supercage structure, cation location (I, II, and III) within X and Y type zeolites. Bottom portion shows the reduction in available space (relative) within supercage as the cation size increases.

of the photobehavior of benzoin alkyl ethers, alkyldeoxybenzoins, and α-alkyldibenzyl ketones included in faujasite-type zeolites (X and Y). The goal of the present investigation is to obtain information concerning the extent of constraints imposed by the zeolite internal structure (surfaces) on the motions of the adsorbed organic molecules and intermediates. In this context, photoreactivity of the above ketones adsorbed on zeolites X and Y has been used as the probe. The knowledge gained through this investigation is expected to be of value in establishing the utility of zeolites as "micro-vessels" for organic reactions.

A brief introduction to the structure, guest location, and mobility of guests within faujasites (a knowledge of which is essential to appreciate the results presented in this report) is provided below. Zeolites are crystalline microporous solids that are widely used as sorbents, ion exchangers, catalysts, and catalyst supports.[5] The primary or "framework" structure of zeolites is based on an infinitely extending three-dimensional network of AlO_4^- and SiO_4 tetrahedra linked to each other by shared oxygen atoms.[6] Each aluminum atom in the network carries a single negative charge that requires an associated cation to maintain electrical neutrality. The unit cell formula of the two types of zeolites, namely, X and Y type, that we have used in this study are as follows:

X type $M_{86}(AlO_2)_{86}(SiO_2)_{106}\cdot 264H_2O$

Y type $M_{56}(AlO_2)_{56}(SiO_2)_{136}\cdot 253H_2O$

where M represents a monovalent cation. As is evident, the two types of zeolites differ mainly in the silicon and aluminum content of the framework and hence the number of counterions. Since the cations in the hydrated case are not "locked in", they are free to move and are exchangeable for other cations. The water can also be displaced without destroying the framework and can be replaced by other molecules whose dimensions are smaller than the pore size of the cavities (vide infra).

The structure of X- and Y-type zeolites consists of an interconnecting three-dimensional network of relatively large spherical cavities, termed supercages (diameter of about 13 Å; Figure 1). Each supercage is connected tetrahedrally to four other supercages through 8-Å windows or pores.[5,6] Supercages are large as evident from their known capacity to include 28 molecules of water, 5.4 molecules of benzene, or 2.1 molecules of perfluorodimethylcyclohexane per cage. Zeolites X and Y also contain, in addition to supercages, smaller cages known as sodalite cages. Sodalite cages are too small to accommodate organic molecules. Charge-compensating cations present in the internal structure of zeolites are known to occupy three different positions in the zeolites X and Y. As illustrated in Figure 1, the first type (site I), 16 in number per unit cell (both X and Y), is located on the hexagonal prism faces between the sodalite units. The second type (site II), 32 in number per unit cell (both X and Y), is located in the open hexagonal faces. The third type (site III), 38 per unit cell in the case of X type and only 8 per unit cell in the case of Y type, is located on the walls of the larger cavity. Only cations of sites II and III are expected to be readily accessible to the adsorbed organic. Free volume available for the organic within the supercage depends on the number and nature of the cation. The free volume decreases by an order of magnitude as the cation size increases from Li to Cs (diameter of Li^+, 1.4; Na^+, 1.9; K^+, 2.7; Rb^+, 3.0; and Cs^+, 3.4 Å; free volume

(2) Turro, N. J.; Wan, P. *Tetrahedron Lett.* **1984**, 3665. Baretz, B.; Turro, N. J. *J. Photochem.* **1984**, *24*, 201. Turro, N. J.; Wan, P. *J. Am. Chem. Soc.* **1985**, *107*, 678. Turro, N. J.; Cheng, C. C.; Lei, X. G.; Flanigen, E. M. *J. Am. Chem. Soc.* **1985**, *107*, 3740. Turro, N. J.; Lei, X. G.; Cheng, C. C.; Corbin, D. R.; Abrams, L. *J. Am. Chem. Soc.* **1985**, *107*, 5824. Lei, X. G.; Dobleday, C. E.; Zimmt, M. B.; Turro, N. J. *J. Am. Chem. Soc.* **1986**, *108*, 2444. Turro, N. J.; Cheng, C. C.; Abrams, L.; Corbin, D. R. *J. Am. Chem. Soc.* **1987**, *109*, 2449. Turro, N. J.; Zhang, Z. *Tetrahedron Lett.* **1987**, *28*, 5637. Turro, N. J.; Fehlner, J. R.; Hessler, D. P.; Welsh, K. M.; Ruderman, W.; Firnberg, D.; Braun, A. *J. Org. Chem.* **1988**, *53*, 3731. Turro, N. J.; Zhang, Z. *Tetrahedron Lett.* **1989**, *30*, 3761.

(3) Casal, H. L.; Scaiano, J. C. *Can. J. Chem.* **1984**, *62*, 628; **1985**, *63*, 1308. Scaiano, J. C.; Casal, H. L.; Netto-Ferreira, J. C. In *Organic Phototransformations in Nonhomogeneous Media*; Fox, M. A., Ed.; American Chemical Society: Washington, DC, 1985; pp 211. Wilkinson, F.; Willsher, C. J.; Casal, H. L.; Johnston, L. J.; Scaiano, J. C. *Can. J. Chem.* **1986**, *64*, 539. Gessner, F.; Olea, A.; Lobaugh, J. H.; Johnston, L.; Scaiano, J. C. *J. Org. Chem.* **1989**, *54*, 259. Benedict, B. L.; Ellis, A. B. *Tetrahedron* **1987**, *43*, 1625. Li, Z.; Wang, C. M.; Persaud, L.; Mallouk, T. *J. Phys. Chem.* **1988**, *92*, 2592. Krueger, J. S.; Mayer, J. E.; Mallouk, T. J. *J. Am. Chem. Soc.* **1988**, *110*, 8232. Persaud, L.; Bard, A. J.; Campion, A.; Fox, M. A.; Mallouk, T. J.; Webber, S. E.; White, J. M. *J. Am. Chem. Soc.* **1987**, *109*, 7309. Dutta, P. K.; Incavo, J. A. *J. Phys. Chem.* **1987**, *91*, 4443. Fox, M. A.; Pettit, T. L. *Langmuir* **1989**, *5*, 1056. Pettit, T. L.; Fox, M. A. *J. Phys. Chem.* **1986**, *90*, 1353. Suib, S. L.; Kostapapas, A. *J. Am. Chem. Soc.* **1984**, *106*, 7705. Liu, X.; Iu, K. K.; Thomas, J. K. *J. Phys. Chem.* **1989**, *93*, 4120.

(4) Corbin, D. R.; Eaton, D. F.; Ramamurthy, V. *J. Am. Chem. Soc.* **1988**, *110*, 4848. Corbin, D. R.; Eaton, D. F.; Ramamurthy, V. *J. Org. Chem.* **1988**, *53*, 5384. Ramamurthy, V.; Corbin, D. R.; Eaton, D. F. *J. Chem. Soc., Chem. Commun.* **1989**, 1213. Ramamurthy, V.; Corbin, D. R.; Eaton, D. F.; Turro, N. J. *Tetrahedron Lett.* **1989**, *30*, 5833. Ramamurthy, V.; Corbin, D. R.; Turro, N. J.; Sato, Y. *Tetrahedron Lett.* **1989**, *30*, 5829. Ramamurthy, V.; Caspar, J. V.; Corbin, D. R.; Eaton, D. F. *J. Photochem. Photobiol. A. Chemistry* **1989**, *50*, 157. Ramamurthy, V.; Corbin, D. R.; Kumar, C. V.; Turro, N. J. *Tetrahedron Lett.* **1990**, *31*, 47. Caspar, J. V.; Ramamurthy, V. Corbin, D. R. *Coord. Chem. Rev.* **1990**, *97*, 225. Ramamurthy, V.; Caspar, J. V. Corbin, D. R. *Tetrahedron Lett.* **1990**, *31*, 1097. Ramamurthy, V.; Caspar, J. V.; Eaton, D. F.; Corbin, D. R.; Kauffman, J.; Dybowski, C. *J. Photochem. Photobiol. A. Chemistry* **1990**, *51*, 259. Ramamurthy, V.; Caspar, J. V.; Corbin, D. R.; Schyler, B.; Maki, A. H. *J. Phys. Chem.* **1990**, *94*, 3391. Ramamurthy, V.; Corbin, D. R.; Turro, N. J.; Zang, Z.; Garcia-Garibey, M. A. *J. Org. Chem.* In Press. Ramamurthy, V. In *Inclusion Phenomena and Molecular Recognition*; Atwood, J. L., Ed.; Plenum Press: New York. In press. Ramamurthy, V.; Caspar, J. V.; Corbin, D. R. *J. Am. Chem. Soc.* In Press.

(5) Turkevich, J. *Catal. Rev.* **1967**, *1*, 1. Weisz, P. B. *Pure. Appl. Chem.* **1980**, *52*, 2091. Flanigen, E. M. *Pure Appl. Chem.* **1980**, *52*, 2191. Smith, J. V. *Chem. Rev.* **1988**, *88*, 149. Holderich, W.; Hesse, M.; Naumann, F. *Angew. Chem., Int. Ed. Engl.* **1988**, *27*, 226. Ozin, G.; Kuperman, A.; Stein, A. *Angew. Chem., Int. Ed. Engl.* **1989**, *28*, 359.

(6) Breck, D. W. *Zeolite Molecular Sieves*; Wiley: New York, 1974. Rabo, J. A., Ed. *Zeolite Chemistry and Catalysis*; American Chemical Society: Washington, DC, 1976. Dyer, A. *Zeolite Molecular Sieves*; John Wiley: New York, 1988.

within the supercage of LiX, 874; NaX, 853; KX, 801; RbX, 771; CsX, 733 Å^3 and LiY, 839; NaY, 832; KY, 812; RbX, 801; CsX, 786 Å^3).

In general, zeolites retain adsorbates by weak intermolecular forces rather than by chemisorption. Such forces control the location and mobility of the included guests within the supercage. Of the various guest molecules, the adsorption of benzene on X- and Y-type zeolites has been followed by infrared,[7] Raman,[8] and UV diffuse reflectance[9] spectroscopies and NMR,[10] neutron diffraction,[11] and other[12] techniques. These studies point toward two locations for adsorbed benzene in the supercage. In the first, a benzene molecule is bound via its π-electrons to the site II sodium ion. In the second location, it is centered in the window formed by the 12-membered oxygen ring between adjacent supercages. The window site is the less stable of the two with proportionately less occupancy at lower coverage. The location of other guest molecules within the supercage is generally speculative and based on the benzene analogy. Motion of organics, especially benzene, included in supercages has been extensively studied by ^{2}H NMR.[13] Generally at room temperature, both rotational and translational motions are restricted within supercages. For example, at low temperatures the only motion of benzene in NaX and NaY is a rotation around the hexad axis; with increasing temperature, jumps between the sites II and the cavities occur. As would be expected the mobility does vary with the organic; for example, the mobility of cyclohexane, cyclohexene, cyclohexadiene, and benzene decreases in the given order. It is generally believed that the dynamic properties of sorbed organics in zeolites are strongly affected by the nature of the counterions. Depending on their size and specific locations, these cations can block the diffusion of the guest molecules to various extents.

The above brief summary shows that supercages of X- and Y-type zeolites are large enough to accommodate a variety of organic molecules of photochemical interest and that they are small enough to provide restrictions on the motions of the included guests. We have been exploring the utility of such confined spaces to alter the reaction paths of photoexcited guest molecules by monitoring the variation in product distribution of a number of photoreactions.[14] In this paper we deal with the photobehavior of benzoin alkyl ethers **1a–d**, alkyldeoxybenzoins **2a–c**, and α-alkyldibenzyl ketones **3a–e**, systems that undergo both Norrish type I and type II reactions. Photolyses of these systems have been extensively studied both in solution[15] and in several other organized media.[16,17] Comparison of product distributions in zeolites with those in isotropic solvents such as benzene, as well as with those in other organized media, we belive, will provide an insight into the extent of restriction offered by the zeolite microporous structure. In this context, this study compliments the recent investigations carried out by Turro and co-workers on dibenzyl ketones adsorbed on faujasite- and pentasil-type zeolites.[2]

Results

General. Photolyses of ketones **1**, **2**, and **3** were conducted while they were adsorbed on the internal microporous structure of zeolites X and Y. The choice of ketones was motivated by the desire to establish the generality of the zeolite effect on the Norrish type I and type II reactions of ketones of widely varying structure. All irradiations were conducted on solvent-free, dry, solid samples. In all cases, the loading level was kept low and it corresponded to an occupancy number of about 0.5 molecules per supercage. Inclusion of ketones within zeolites was achieved by using hexane as the solvent. Generally products were extracted with ether after about 2 h of photolysis (<15% conversion, similar conversion was obtained in benzene in about 15 min). In each case, one experiment was conducted in which the products were isolated by dissolving the zeolite framework with concentrated HCl followed by extraction with ether. Product distributions obtained by these two methods (ether extractions with and without acid) were identical within 5%. Material balance in general was ~90%. These protocols ensured that no unidenified products were trapped within the zeolite framework. Products were analyzed by gas chromatography using *trans*-stilbene as the internal standard. For comparison, irradiation was also conducted in benzene in the absence of zeolite. Product distributions for **1**, **2**, and **3** in benzene are close to the literature values.[15-17]

Benzoin Alkyl Ethers. Photolyses of benzoin alkyl ethers **1a–d** in nitrogen-saturated benzene give benzil and pinacol ethers, derived via the type I pathway, as major products along with deoxybenzoin and the corresponding cyclobutanols, derived via the type II process, as minor products (Scheme I, where X = O). In contradistinction, irradiation of these adsorbed on the internal surfaces of the X- and Y-type zeolites gives benzoylbenzyl alkyl ether (**4**, where X = O, in Scheme I) as the major product, a product that was only very minor in benzene. The yield of this product was very dependent on the nature of the cation present within the zeolite supercage. In addition to such a dramatic change in the products obtained via the type I process, the relative yield of type II products also

(7) Angell, C. L.; Howell, M. V. *J. Colloid. Interfac. Sci.* **1968**, *28*, 279. Coughlan, B.; Carroll, W. M.; O'Malley, P.; Nunan, J. *J. Chem. Soc., Faraday Trans. 1* **1981**, *77*, 3037. de Mallmann, A.; Barthomeuf, D. *Zeolites* **1988**, *8*, 292.

(8) Freeman, J. J.; Unland, M. L. *J. Catal.* **1978**, *54*, 183.

(9) Unland, M. L.; Freeman, J. J. *J. Phys. Chem.* **1978**, *82*, 1036. Primet, M.; Garbowski, E.; Mathieu, M. V.; Imelik, B. *J. Chem. Soc., Faraday Trans. 1* **1980**, *76*, 1942.

(10) Nagel, M.; Michel, D.; Geschke, D. *J. Colloid. Interfac. Sci.* **1971**, *36*, 254. Borovkov, V.; Yu.; Hall, W. K.; Kazanski, V. B.; *J. Catal.* **1978**, *51*, 437. Ryoo, R.; Liu, S. B.; de Menorval, L. V.; Takegoshi, K.; Chmelka, B.; Trecoske, M.; Pines, A. *J. Phys. Chem.* **1987**, *91*, 6575.

(11) Fitch, A.; Jobic, H.; Renouprez, A. *J. Phys. Chem.* **1986**, *90*, 1311. Jobic, H.; Renouprez, A.; Fitch, A.; Lauter, H. J. *J. Chem. Soc., Faraday Trans. 1* **1987**, *83*, 3199. Czjzek, M.; Vogt, T.; Fuess, H. *Angew. Chem., Int. Ed. Engl.* **1989**, *28*, 770.

(12) Demontis, P.; Yashonath, S.; Klein, M. L. *J. Phys. Chem.* **1989**, *93*, 5016.

(13) Lechert, H.; Haupt, W.; Wittern, K. P. *J. Catal.* **1976**, *43*, 356. Lechert, H.; Basler, W. D. *J. Phys. Chem. Solids* **1989**, *50*, 497. Boddenberg, B.; Burmeister, R.; Spaeth, G. In *Zeolites as Catalysts, Sorbents and Detergent Builders*; Karge, H. G., Weitkamp, J., Eds.; Elsevier: Amsterdam, 1989; pp 533–543.

(14) Ramamurthy, V.; Eaton, D. F. *Acc. Chem. Res.* **1988**, *21*, 300. Syamala, M. S.; Devanathan, S.; Ramamurthy, V. *Proc. Indian Acad. Sci.* **1987**, *98*, 391. Ramamurthy, V.; Venkatesan, K. *Chem. Rev.* **1987**, *87*, 433.

(15) Lewis, F. D.; Lauterbach, R. L.; Heine, H. G.; Hartmann, W.; Rudolph, H. *J. Am. Chem. Soc.* **1975**, *97*, 1519. Heine, H. G.; Hartmann, W.; Kory, D. R.; Magya, J. G.; Hoyle, C. E.; McVey, J. K.; Lewis, F. D. *J. Org. Chem.* **1974**, *39*, 691. Lewis, F. D.; Hoyle, C. E.; Magyar, J. G.; Heine, H. G.; Hartmann, W. *J. Org. Chem.* **1975**, *40*, 488.

(16) de Mayo, P.; Nakamura, A.; Tsang, P. W. K.; Wong, S. K. *J. Am. Chem. Soc.* **1982**, *104*, 6824. de Mayo, P.; Ramnath, N. *Can. J. Chem.* **1986**, 64, 1293. Tomioka, H. S.; Izawa, Y. *J. Chem. Soc., Chem. Commun.* **1980**, 445.

(17) Dasaratha Reddy, G.; Usha, G.; Ramanathan, K. V.; Ramamurthy, V. *J. Org. Chem.* **1986**, *51*, 3085. Dasaratha Reddy, G.; Ramamurthy, V. *J. Org. Chem.* **1987**, *52*, 5521. Dasaratha Reddy, G.; Ramamurthy, V. *J. Org. Chem.* **1987**, *52*, 3952. Devanathan, S.; Ramamurthy, V. *J. Phys. Org. Chem.* **1988**, *1*, 91. Nageswer Rao, B.; Syamala, M. S.; Turro, N. J.; Ramamurthy, V. *J. Org. Chem.* **1987**, *52*, 5517.

Scheme I. Pathways to Products upon Photolysis of Benzoin Alkyl Ethers and α-Alkyldeoxybenzoins

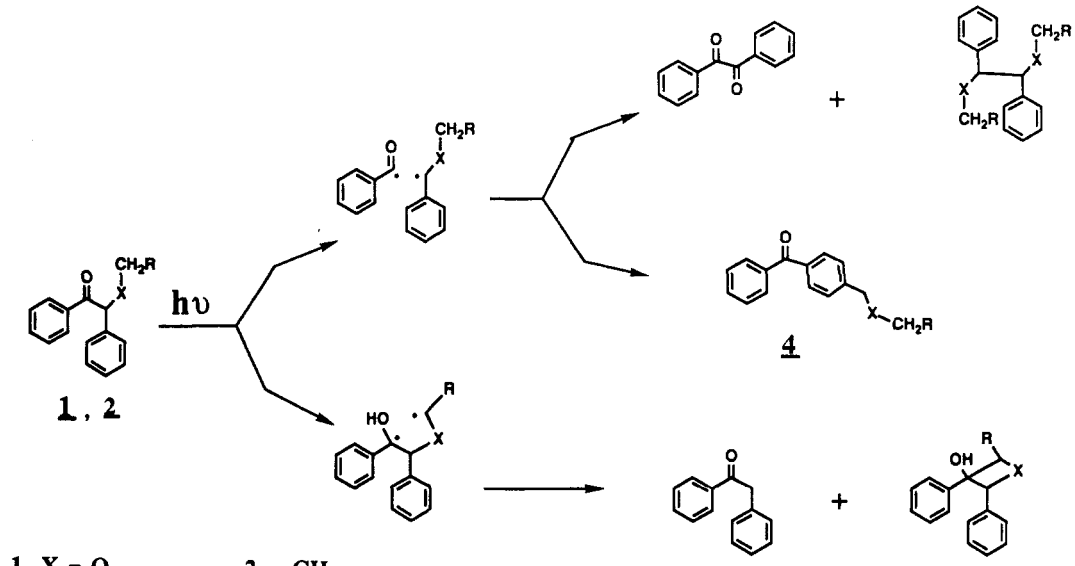

increased with respect to benzene. More importantly, the relative amount of cyclobutanol was dependent on the size of the cation present within the supercage. These results are summarized in Table I. Also, note that the cation effect on product distribution was much less in Y-type zeolites than in X-type zeolites for smaller alkyl chain ethers.

α-Alkyldeoxybenzoins. As observed in the case of benzoin alkyl ethers, the photobehavior of α-alkyldeoxybenzoins **2a–c** differed significantly when included in X- and Y-type zeolites compared to that in benzene. As shown in Table II, α-alkyldeoxybenzoins when photolyzed in benzene give benzil and diphenylalkanes as type I products and deoxybenzoin and the corresponding cyclobutanols as type II products (Scheme I, where X = CH_2). Remarkably, these alkyldeoxybenzoins exhibited significantly different behavior when included in zeolites. The rearrangement product, *p*-alkylbenzophenone (**4**, where X = CH_2 in Scheme I) derived via the type I pathway, was obtained as a major product. In LiX this is obtained in over 90% yield. Enhancement of the rearrangement process at the expense of normal coupling products is common for both benzoin alkyl ethers and alkyldeoxybenzoins. Another common behavior to be noted is the relative ratio of products obtained via cyclization and elimination of the type II 1,4-diradical: the cyclization process is enhanced within the zeolite supercage, especially in the presence of larger cations.

α-Alkyldibenzyl Ketones. Photolyses of α-alkyldibenzyl ketones **3a–e** in benzene and as inclusion complexes of X and Y zeolites give products resulting from the Norrish type I and type II reactions (Scheme II). Results from these ketones are summarized in Tables III and IV. There are remarkable differences in product distribution between benzene solution (Table IV) and the solid zeolite complexes (Table III). Within the zeolite, the main products are 1,2-diphenyl-1-alkylethanes (**5**, AB), 1-phenyl-4′-alkylacetophenones (**6**), and olefins, whereas in benzene both olefins and **6** are absent. The yields of both

Table I. Product Distribution upon Photolysis of Benzoin Alkyl Ethers within Zeolites[a–c]

	type I products		type II products	
medium	benzil/pinacol ether	rearrangement product	deoxybenzoin	cyclobutanol
	Benzoin Methyl Ether (1a)			
benzene	26/67	1.0	1	7
LiX	3	77	13	8
NaX	4	72	10	14
KX	7	48	14	18
RbX	5	46	18	22
CsX	8	34	17	31
NaY		61	33	6
KY		64	24	12
RbY		68	18	12
CsY		67	17	14
	Benzoin Ethyl Ether (1b)			
Benzene	31/64	0.5	0.4	5
LiX	2/3	74	15	6
NaX	4/7	65	14	10
KX	8/5	39	27	24
RbX	8/9	19	23	30
	Benzoin Hexyl Ether (1c)			
Benzene	10/76	2.5	6	6
LiX		98	1	1
NaX		92	3	4
KX		68	7	24
RbX		49	12	38
	Benzoin Octyl Ether (1d)			
Benzene	16/75		1	8
LiX		83	13	3
NaX		80	14	7
KX		58	23	18
RbX		46	20	33
NaY		89	10	1
KY		80	8	12
RbY		66	8	25

[a] See Scheme I for products. [b] Numbers reported are average of at least four independent runs. Product yields were measured at ~15% conversion by gas chromatography with *trans*-stilbene as the internal standard. [c] For details on loading levels, extraction procedure, etc., see Experimental Section.

Scheme II. Pathways to Products upon Photolysis of α-Alkyldibenzyl Ketones

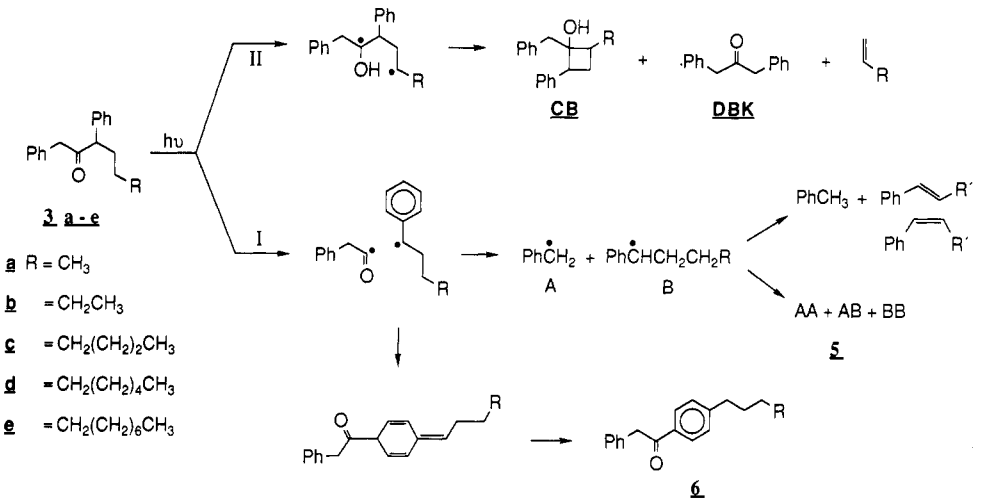

Table II. Product Distribution upon Photolysis of Alkyldeoxybenzoins within Zeolites[a-c]

	type I products		type II products	
medium	benzil/pinacol ether	rearrangement product	deoxybenzoin	cyclobutanol
	α-Propyldeoxybenzoin (**2a**)			
benzene	5/24		54	17
LiX		95	4	1
NaX		88	5	7
KX		48	31	21
RbX		32	22	45
CsX		21	27	42
LiY		76	15	10
NaY		64	12	23
KY		34	10	56
RbY		20	19	61
CsY		6	16	78
	α-Butyldeoxybenzoin (**2b**)			
Benzene	5/30		44	21
LiX		90	6	4
NaX		82	9	9
KX		52	21	26
RbX		43	21	34
CsX		28	25	46
LiY		91	6	3
NaY		69	17	14
KY		41	13	46
RbY		21	22	57
CsY		8	16	76
	α-Octyldeoxybenzoin (**2c**)			
Benzene	6/45		24	21
LiX		97	3	
NaX		80	6	14
KX		50	14	35
RbX		36	13	51
LiY		96	4	
NaY		85	11	4
KY		52	9	39
RbY		41	16	42

[a] See Scheme I for products. [b] Numbers reported are average of at least four independent runs. Product yields were measured at ~15% conversion by gas chromatography with *trans*-stilbene as the internal standard. [c] For details on loading levels, extraction procedure, etc., see Experimental Section.

olefins and **6** are dependent on the nature of the cation present inside the supercages of X zeolites. As the cation size increases (Li^+ to Cs^+), the yield of **6** decreases and that of olefin increases at the expense of **5**.

Discussion

Inclusion of Organics within Zeolites. Laboratory samples of zeolites X and Y are hydrated as such and the supercages are filled with water. In general, these fail to include organics both from solution and from vapor phase. Therefore, the cages need to be emptied and this is achieved by activating the zeolite at 500 °C for about 6 h in an aerated medium. During this process, water present in the interior of the zeolite is evaporated off without any other structural changes taking place. Such activated zeolites are used as the "host" in the present study. Although the majority of early studies (mostly physical) on zeolites adopted vapor-phase (vacuum line) techniques to include molecules within zeolites, we have found it convenient to use solution methods for routine studies. Only when the ambient humidity was high (>85%), did we use a drybox; otherwise, all operations were carried out under normal laboratory conditions. Under such conditions, we found that it required about 24 h for activated X and Y zeolites to readsorb water to its full capacity (~22% by weight) while kept on the pan of a Mettler balance. Nonpolar solvents such as hexane, pentane, and cyclohexane were found to be the best solvents from which the ketones are readily incorporated into the zeolites. Ketones, having lesser affinity for nonpolar solvents, readily distributed themselves into the zeolite while the solvent showed poor affinity for the zeolite interior as compared to the ketones **1**, **2**, and **3**. When solvents such as ether and benzene were used, they competed for the interior sites and displaced the ketones. Also, ketones showed less preference for the zeolite interior over the external polar medium. In fact, such a difference in behavior enabled us to use nonpolar hexane to include the reactants into the supercage and polar ether to exclude/extract the products from the interior of the zeolites. All irradiations were conducted under degassed conditions on dry samples, obtained by including the ketones **1**, **2**, and **3** from hexane solution and by drying under reduced pressure (10^{-4} mm). Better reproducible samples are obtained by annealing the above-dried samples at ~60 °C for about 3 h. Furthermore, samples needed to be dried thoroughly as the presence of even small amounts of residual solvent altered the product distribution. Finally, the occupancy number, $\langle S \rangle$ (the number of molecules included/number of available supercages), was kept constant at ~0.5. Variation of $\langle S \rangle$ may have consequences on product distribution and this aspect was not investigated.

Interpretation of Results. As illustrated in Schemes I and II, products formed from **1**, **2**, and **3** can be understood on the basis of the type I and type II reactions.

Table III. Product Distribution[a] upon Photolysis of α-Alkyldibenzyl Ketones within Zeolites[b-d]

	α-propyldibenzyl ketone (3a)			α-butyldibenzyl ketone (3b)			α-hexyldibenzyl ketone (3c)			α-octyldibenzyl ketone (3d)			α-decyldibenzyl ketone (3e)		
medium	olefin	5 (AB)	6	olefin	5 (AB)	6	olefin	5 (AB)	6	olefin	5 (AB)	6	olefin	5 (AB)	6
LiX	16	24	47	25	16	59	39	17	37	48	11	41	56	8	36
NaX	17	30	38	17	18	63	19	18	57	26	23	51	42	17	41
KX	26	39	19	27	19	54	23	29	36	26	23	51	42	17	41
RbX	42	20	27	50	13	37	38	23	29	51	24	25	61	12	27
CsX	46	16	35	56	10	34	60	15	22	65	20	14	78	7	14
LiY	15	55	15	16	60	24	26	44	23	17	40	42	34	44	18
NaY	16	61	12	24	48	29	26	43	25	26	40	34	20	56	24
KY	10	73	6	12	71	17	22	54	20	17	63	19	17	60	20
RbY	11	75	8	15	65	20	21	52	22	26	53	22	22	55	22
CsY				26	51	18	35	39	19	36	42	23	39	44	18

[a] See Scheme II for products. [b] Numbers reported are average of at least four independent runs. Product yields were measured at ~15% conversion by gas chromatography with *trans*-stilbene as the internal standard. [c] For details on loading levels, extraction procedure, etc. see Experimental Section. [d] In all cases type II products, dibenzyl ketone and the corresponding cyclobutanols, were formed in about 10% yield. Their yields were not significantly dependent on the cations.

Table IV. Product Distribution upon Photolysis of α-Alkyldibenzyl Ketones in Benzene[a]

		type I products			type II products	
ketone	olefin	5 (AA)	5 (AB)	5 (BB)	cyclobutanol	dibenzyl ketone
α-propyl-DBK[c]	3	21	43	21	9	3
α-butyl-DBK	2	20	42	22	9	3
α-hexyl-DBK	4	17	36	18	13	4
α-octyl-DBK	4	18	40	19	9	3
α-decyl-DBK	5	19	40	20	10	4

[a] See Scheme II for products. [b] Numbers reported are average of at least four independent runs. Product yields were measured at ~15% conversion by gas chromatography with *trans*-stilbene as the internal standard. [c] Dibenzyl ketone represented as DBK.

Although some of the products formed in zeolites are significantly different from those formed in solution, these have been reported earlier as products in other organized/confined media.[16,17] The present investigation utilizes the photobehavior of **1**, **2**, and **3** as probes of the internal microporous structure of zeolites to get information regarding the nature of zeolite–organic interaction. Two aspects of the results are valuable in this context: variation of product distribution in zeolites with respect to that in benzene and variation in product distribution between various cation-exchange zeolites. Both aspects, we believe, reflect the restriction imposed by the zeolite internal structure on the motions of the reactive ketones and the intermediates therefrom, namely, the type I radical pairs (primary and secondary) and the type II 1,4-diradical. Results are discussed below on the basis of the effect of zeolite–guest interactions on intercage migration, intracage motions, and intramolecular rotations of the above species.

In order to interpret the results, one needs to have some knowledge about the location of the guest ketones when they are adsorbed onto zeolites. Of the two possible locations—internal and external surfaces—we believe that the adsorption occurs on the internal surface for the following reasons. (a) The available external surface area is much smaller (<1%) compared to the internal surface area. (b) No significant amount of ketones are adsorbed onto zeolites with too small a pore diameter to admit these molecules (e.g., zeolites 4A and 5A). (c) The photochemical behavior of **1**, **2**, and **3** within zeolites X and Y was significantly different from that on silica gel (had the molecules been adsorbed onto the external surface of zeolites X and Y, one might anticipate behavior similar to that on silica gel surface). (d) The adsorption isotherm measured for benzoin methyl ether suggests that the maximum amount of guest adsorbed is related to the internal free volume (the internal free space as well as the maximum amount of ketone adsorbed decreases in the order LiX, KX, and CsX).

The interior of zeolites X and Y contains both supercages and sodalite cages. Of these, sodalite cages are too small to accommodate these ketones. From molecular modeling studies, it was clear that all three types of ketones can fit within either a single supercage or between two supercages. Once the ketones are in these locations they would be close to the cation. Indeed, thermogravimetric analyses results indicate the presence of an interaction between the cation and the ketone. The temperature of desorption of benzoin methyl ether, α-propyldeoxybenzoin, and α-hexyldibenzyl ketone adsorbed over LiY, KY, and CsY were as follows: benzoin methyl ether, LiY, 514; KY, 491; CsY, 455 °C; α-propyldeoxybenzoin, LiY, 421; KY, 396; CsY 389 °C; α-hexyldibenzyl ketone, LiY, 428; KY, 417; CsY, 381 °C. It is known that the stronger the interaction between the cation and the adsorbent, the higher the desorption temperature would be. Among Li^+, K^+, and Cs^+, the strength of interaction would decrease in that order.[7-9,18] The temperature of desorption measured for all three ketones by TGA technique also decreases in the order of expected binding strength. Thus, we believe that the location of the reactive ketones is within the internal surface of zeolites and in proximity to the cation located within the supercage.

Restriction of Intercage Translational Migration. X and Y zeolites have a three-dimensional structure with all the supercages interconnected. Molecules and intermediates accommodated in one supercage should in principle be able to migrate to adjacent cages. The extent and the facility with which they can migrate will determine the products formed in most fragmentation and bimolecular reactions. Although information on molecular migration on zeolite internal surfaces is available, they all relate to simple hydrocarbons and aromatics such as hexane and benzene.[19] Therefore, to obtain information on molecules of organic chemists' interests, we have utilized photoreactions as probes. In this context, we believe that in-

(18) Tsitsishvili, G. V.; Andronikashvili, T. G. In *Molecular Sieve Zeolites*; Flanigen, E. M., Sand, L. B., eds., American Chemical Society: Washington, DC, 1971; pp 217–228. Avgul, N. N.; Bezus, A. G.; Dzhigit, O. M. In *Molecular Sieve Zeolites*; Flanigen, E. M., Sand, L. B., Eds.; American Chemical Society: Washington, DC, 1971; pp 184–192. Bertsch, L.; Habgood, H. W. *J. Phys. Chem.* **1963**, *67*, 1621.

(19) Pfeifer, H. *Phys. Rep.* **1976**, *26*, 293. Barrer, R. M. *Adv. Chem.* **1971**, *102*, 1. Karger, J.; Ruthven, D. M. *Zeolites* **1989**, *9*, 267.

formation concerning the translational motion (intercage migration) of organics within the zeolite internal surfaces is provided by the pathways undertaken by the geminate radical pairs generated by photofragmentation (Norrish type I) of ketones **1**, **2**, and **3** (Schemes I and II). In isotropic media, the fragments of the α-cleavage process, benzoyl and benzyl radicals in the case of **1** and **2**, are free to diffuse away, resulting in coupling reactions to yield benzil, pinacol ethers, and diphenylalkanes (Scheme I). It is clear from Tables I and II that in zeolites these radical pairs pursue a different pathway, namely, recombination with rearrangement to give benzoylbenzyl alkyl ether (from **1**) and *p*-alkylbenzophenone (from **2**; **4** in Scheme I). Also normal coupling products benzil, pinacol ethers, and diphenylalkanes are generally absent and are only minor in the case of **1a** and **1b**. These differences in behavior between isotropic solvents and zeolites, we believe, suggest that the geminate radical pair's translational mobility is restricted by the internal surfaces of the zeolite and radicals are forced to undergo in-cage recombination. These observations lead one to conclude that between the intracage geminal recombination (with or without rearrangement) and migration to adjacent cages, the latter is slow. From Table I, it is obvious that when the alkyl chain is longer, no benzil and pinacol ethers are obtained in any zeolites, indicating that addition of a longer α-alkyl chain hinders the translational motion even further.

The above conclusions are also supported by the results with α-alkyldibenzyl ketones (Table III). In this system information regarding translational motion of adsorbed organics is provided by the pathways undertaken by both the primary and the secondary radical pairs (Scheme II). The primary triplet radical pair generated by α-cleavage, in the absence of any significant cage effect, is known to diffuse apart and decarbonylate.[20] However, within zeolites this is not the case. The rearrangement to yield *p*-alkylacetophenones (**6** in Scheme II) is preferred. This suggests that diffusion to adjacent cages is slow compared to the decarbonylation. This conclusion is further supported by the fact that in all cases the coupling product **5** (AB) alone is obtained from the secondary radical pair; this requires the decarbonylation to occur in the presence of the benzyl radical, a member of the primary radical pair. If one were to assume that a primary radical's lifetime is controlled essentially by the decarbonylation process occurring at a rate[21] of 10^7 s^{-1}, movement to adjacent cages, if it occurs, should be on a time scale longer than 10^{-7} s. From the above results as well as from those of Turro and co-workers,[2] it is clear that translational mobility of organics is significantly reduced on the internal surfaces of zeolites. Such restrictions can be utilized to control or alter the behavior of an excited molecule and the intermediates derived therefrom.

Restriction of Intracage Motions. One rarely considers potential restriction of molecular motions during unimolecular reactions in isotropic nonpolar solvents. However, in media where there are weak interactions between the reactant and the media, such interactions (frictions) can become critical and may even determine the pathways undertaken by the reactants or intermediates. Reactants included in supercages of X and Y zeolites are expected to interact with the walls of the cavity and with the cations present therein. Furthermore, the fit inside the supercage may become tight, depending on the sizes

Scheme III. Possible Termination Processes for Benzyl Radical Pair within a Supercage. Three Orientations for Radical Pair Are Shown; It Is Not Clear Which One of These Would be Generated upon Cleavage

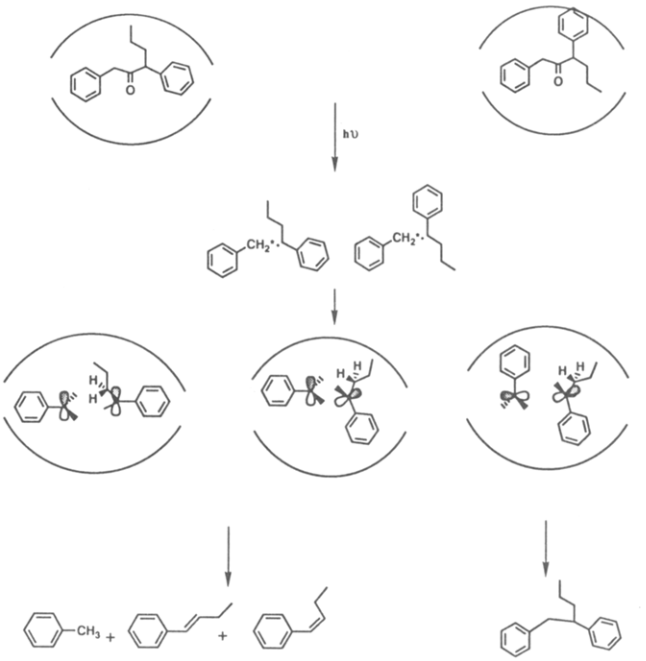

of the guest and the cation. Such a tight fit and interactions between the host and the guest would be expected to restrict the motions of guests within supercages. In order to predict the reactivity pattern of the guest molecule, one needs to have some information on the extent of available freedom of motion for the guest molecules within the supercage. Current knowledge, based on ^2H NMR, is restricted to simple aromatic molecules.[13] We illustrate below that photochemical reactions can serve as simple probes to obtain such information for molecules of general organic interest.

Information on the restriction of intracage motions of the supercage-included molecules is provided by variation in the product distribution derived from processes occurring within a single cage. In this context, unequivocal information regarding the restriction of motions of supercage-included guests is provided by the behavior of the benzylic secondary radical pair derived from **3** (Scheme III). In solution, the termination process consists only of the coupling between the two benzylic radicals and results in diphenylalkanes AA, AB, and BB (**5** in Scheme II) in a statistical ratio of 1:2:1 (Table IV). The alternate pathway, disproportionation, which is common for alkyl radical pairs, is rarely observed in solution for benzylic radical pairs. Within supercages, termination proceeds by both coupling and disproportionation (Table III). A schematic diagram for the termination processes between the benzylic radicals is shown in Scheme III. It has been suggested[22] that the reason for the reactivity differences between alkyl and benzylic radical pairs is that the latter can form dimeric association complexes that can easily collapse to coupling products but whose geometry is unfavorable for disproportionation.

We interpret the preference for disproportionation within the supercage as follows. The association between benzylic radicals mentioned above would be prohibited inside the cavity, especially in the presence of large cations

(20) Engel, P. S. *J. Am. Chem. Soc.* **1970**, *92*, 6074. Robbins, W. K.; Eastman, R. H. *J. Am. Chem. Soc.* **1970**, *92*, 6076.
(21) Lehr, G. F.; Turro, N. J. *Tetrahedron* **1981**, *37*, 3411. Brunton, G.; McBay, H. C.; Ingold, K. U. *J. Am. Chem. Soc.* **1977**, *99*, 4447.
(22) Neuman, R. C.; Alhadeff, E. S. *J. Org. Chem.* **1970**, *35*, 3401. Kopecky, K. R.; Yeung, M. *Can. J. Chem.* **1988**, *66*, 374.

Scheme IV. Relationship between the Free Volume within a Supercage and Possible Restrictions on Molecular Motions within a Supercage. As the Cation Size Increases Free Volume within a Supercage Decreases (Not to Scale)

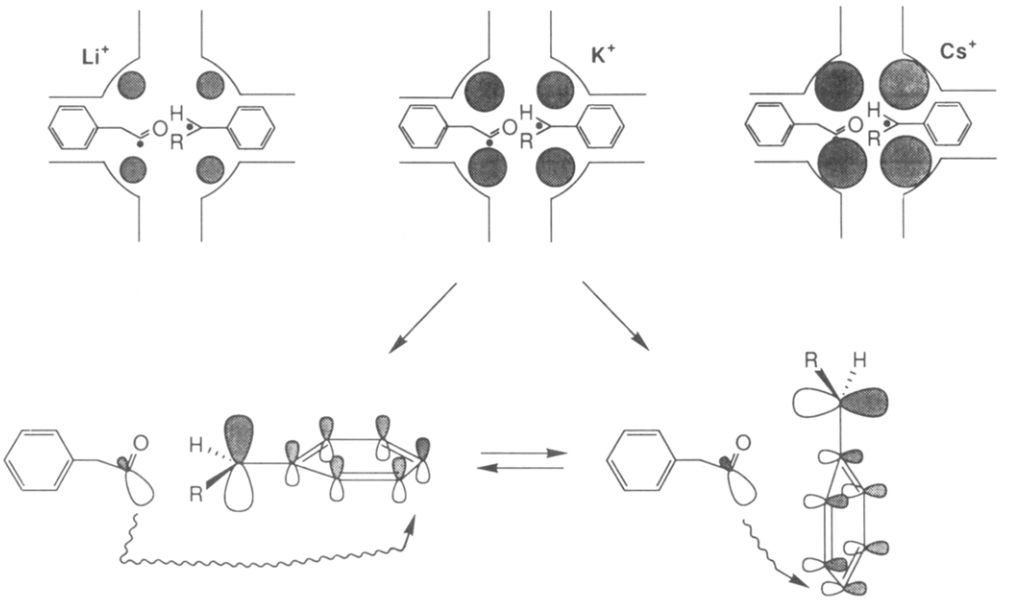

due to reduction in free volume (see Introduction section). Further, more drastic overall motion would be required to bring benzylic radicals together for head-to-head coupling than to move an alkyl group so that one of its methylene hydrogens would be in a position for abstraction by the benzylic carbon radical. It is logical to expect the radical pair to prefer the pathway of "least motion" when the free space around them is small. Thus, as smaller cations are replaced with larger ones and as shorter alkyl chains are replaced with longer ones, one would indeed expect enhanced yields of olefins as observed in the present study. These results clearly suggest that the motion of the radical pair is restricted within the supercage and that the extent of restriction, as would be expected, is directly related to the available free volume within the supercage.

The above conclusion is also supported by the pathways undertaken by the primary triplet radical pair (Scheme II) generated by α-cleavage of **3**. Information concerning the intracage motional restriction, we believe, is provided by the variation in the relative yield of the rearrangement product with respect to the cation. As discussed above, occurrence of the rearrangement process (which is absent in isotropic solvents) is a consequence of the restriction imposed by the zeolite pores on intercage migration of primary radical pair. Perusal of Table III reveals that while the rearrangement takes place in all cation-exchanged X and Y zeolites, the yield of the rearrangement product **6** varys depending on the cation. The yield decreases as the cation present in the supercage is changed from Li^+ to Cs^+. Such a trend, we believe, is a consequence of the decrease in the free space within the supercage. As the available free space inside the supercage is decreased by the increase in the size of the cation, the translational and rotational motions required for the rearrangement process become increasingly hindered (Scheme IV). Under these conditions, competing paths such as coupling, to yield the starting ketone, and decarbonylation, both of which require little motion, dominate.

The above interpretation assumes that the variation in the yield of the rearrangement product is not due to any other mechanistic features. The reduction in yield could come from the dependence of the rate or efficiency of type I cleavage and/or type II processes on the cation. Since the yield of type II products in the case of **3** did not change significantly with the cation, our conclusions based on this system are expected to be valid.[23]

Restriction of Intramolecular Rotations within a Supercage. From the above discussion it is clear that there are some restrictions on inter- and intracage molecular motions of supercage-included guests. In addition to inter- and intracage motions, chemical reactions involve intramolecular bond rotations and group/atom migrations. We note that such intramolecular single-bond rotations may also become restricted within the supercage. The partitioning of the type II 1,4-diradical derived from both **1** and **2** provides information concerning such intramolecular rotational restriction imposed by the supercage on the included guests. Inspection of Tables I and II reveals that both the extent of participation of type II process (type I to type II ratio) and the ratio of cyclobutanol (resulting from cyclization, C, of the type II 1,4-diradical) to deoxybenzoin (result of elimination process, E, from the 1,4-diradical) depend on the zeolite used. Stereochemistry of cyclobutanols are not known and therefore additional information based on the variation of cyclobutanol isomers could not be obtained. In this section we concern ourselves with the variation of C/E with the zeolite used.

The Norrish type II reaction of ketones has been extensively investigated and the mechanistic details are fairly well understood.[24] The triplet 1,4-diradical, the primary intermediate, is generated in the skew form (**7** in Scheme V) but readily transforms to the transoid (**8**) and the cisoid (**9**) conformers via a rotation of the central σ-bond. As illustrated in Scheme V, these conformers undergo further reaction to yield cyclobutanol, olefin, and enol as final products. Under the restricted/confined situations, the decay occurs directly from the skewed conformer. While both the cisoid and skewed conformers decay to the final products via both the elimination and cyclization processes,

(23) If the type I and/or type II reactivities are affected by the presence of cation, the total yield of type I and type II products will depend on the cation. This seems to happen in the case of 1 and 2. We believe that smaller cations Li^+ and Na^+ enhances the type I reactivity. This aspect will be discussed with more examples in a future article.

(24) Wagner, P. J. *Acc. Chem. Res.* **1971**, 4, 168. Turro, N. J.; Dalton, J. C.; Dawes, K.; Farrington, G.; Hautala, R.; Morton, D.; Niemczyk, M.; Schore, N. *Acc. Chem. res.* **1971**, *5*, 92. Scaiano, J. C. *Acc. Chem. Res.* **1982**, *15*, 252.

Scheme V. Mechanistic Scheme for Norrish Type II Reactions of Ketones. Type II Radicals from Benzoin Systems within a Supercage Are Shown on Bottom

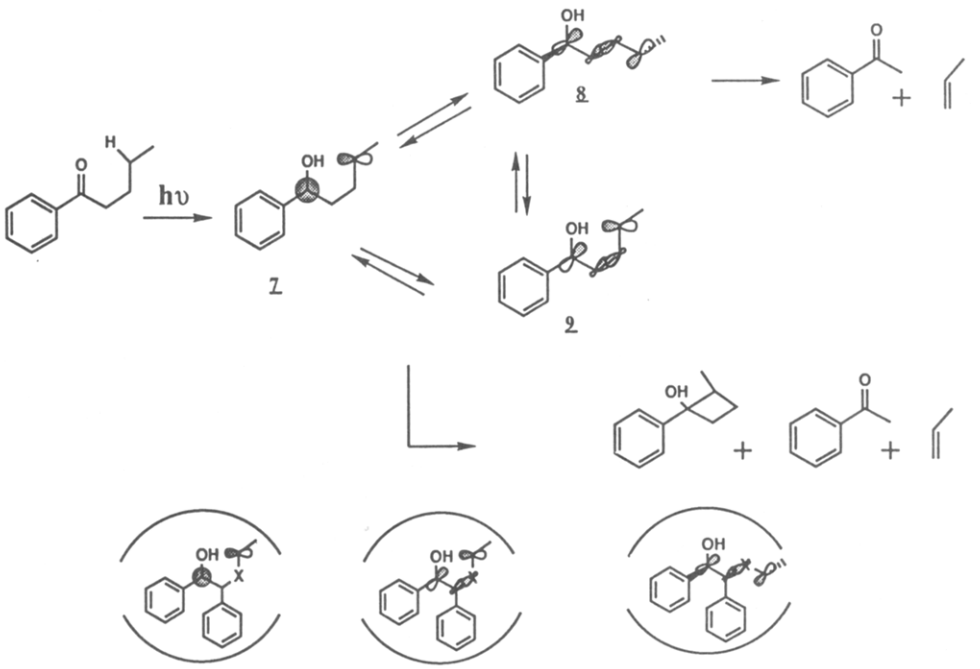

the transoid conformer undergoes only the fragmentation reaction. The fragmentation process from the cisoid and skewed conformers is controlled by the extent of overlap of the singly occupied p orbital with the central σ-bond. In the absence of a good overlap, cyclization is preferred.[25] Product formation is preceded by intersystem crossing of the triplet to the singlet diradical. From the above established mechanistic features, it is clear that one can understand the influence of the supercage on the cyclization to elimination yield on the basis of its effect on the equilibrium distribution of the cisoid, transoid, and skewed conformers, on the feasibility of overlap of the p orbital with the central σ-bond, and on triplet–singlet intersystem crossing of the 1,4-diradical.

Examination of Tables I and II reveals that in all the ketones investigated the C/E ratio, i.e., the ratio of the yield of the cyclobutanol, the cyclization product of γ-hydrogen abstraction process, to that of deoxybenzoin, the elimination product, depends on the cation present in the supercage. Also, the C/E ratio increases as smaller cations are replaced with larger ones, i.e., C/E increases from Li^+ to Cs^+. The enhancement of cyclization within the supercages of X and Y zeolites in the presence of larger cations, we propose, reflects the rotational restriction brought on the skewed–transoid–cisoid diradical interconversion. It is known that in a medium where the 1,4-diradical is hydrogen bonded, the diradical prefers a transoid geometry and therefore elimination products dominate the product mixture. Similar weak electronic interaction is also expected between the cation and the 1,4-diradical intermediate, and such interaction would favor the transoid conformer for the 1,4-diradical. Higher contributions of the transoid conformer in the equilibrium would enhance the yield of elimination products. On the basis of this model, one would expect the yield of elimination product to depend on the binding strength of the cation with the intermediate 1,4-diradical. Indeed a higher yield of elimination product is obtained with smaller cations, which are expected to bind more strongly. We do not believe that this alone is responsible for the observed enhancement of cyclization product with Rb^+ and Cs^+ as cations. In addition to the electronic effect mentioned above, a steric effect also plays a major role in controlling the product ratio. We propose that as the cation size increases, the 1,4-diradical is forced to adopt a compact geometry due to reduction in the available supercage free volume. Thus the first-formed skewed 1,4-diradical would be encouraged to relax to the cisoid rather than to the transoid conformer. Severe constraints would be imposed by the supercage on the cisoid–transoid interconversion and the barrier for the cisoid to transoid conversion would be accentuated. These factors would be expected to enhance the yield of cyclobutanol. Indeed these predictions are realized in the case of zeolites containing larger cations (Tables I and II). Therefore, the dependence of the C/E ratio on the cation can be attributed to the electronic and steric controlled restriction of intramolecular rotation of the C–C bonds by the cations present within the supercage.

Conclusions

This study has elucidated some of the features of the internal surfaces of zeolites as revealed by their influence on the prototypical photoreactions of excited ketones. Although this study is restricted to ketones, the knowledge gained here is expected to be of general value. Interactions between the host zeolite and the guest ketones restrict the translational motion of molecules on the internal surfaces of zeolites. Such reduction in translational motion on silica surfaces has been reported earlier.[26] Although diffusional rates on zeolite internal surfaces for molecules of organic interest are not measured, molecular migration on zeolite internal surfaces is expected to be slower than on silica surfaces due to the presence of cations. Molecular rotation and migration within the supercage is also restricted. In addition, intramolecular rotation of certain C–C bonds is

(25) For mechanistic conclusions based on crystal structure studies, see: Ariel, S.; Evans, S. V.; Garcia-Garibay, M.; Harkness, B. R.; Omkaram, N.; Scheffer, J. R.; Trotter, J. *J. Am. Chem. Soc.* **1988**, *110*, 5591.

(26) de Mayo, P.; Johnston, L. J. In *Preparative Chemistry Using Supported Reagents*; Laszlo, P., Ed. Academic: New York, 1987; pp 61–75.

also restrained to some degree.

Various organized and confined structures such as crystals, organic hosts (cyclodextrin, deoxycholic acid, Dianin's compound), micelles, liquid crystals, and silica surfaces have been explored as media for photoreactions.[1] Each one of them possess unique features. Zeolites compare favorably with these as media for photoreactions. One of the disadvantages in using zeolites, like most other solid matrices, as the media can be the long duration (compared to solution) of irradiation required because of scattering problems. Also, one needs to continuously expose fresh surfaces to UV radiation through mechanical agitation. In spite of these drawbacks, zeolites should not be overlooked as a medium for photoreactions since we and others have successfully conducted photochemical and photophysical studies in this media.[2-4] Compared to most of the organic hosts, inclusion of a large variety of guests within zeolites is easily achieved. Zeolites are unique, stable, and photoinert host materials with well-defined pore structures that can offer predictable constraints on the motions of included guests which can be used to direct the probable course of the photoreactions within them.

Experimental Section

Materials. Benzoin alkyl ethers and alkyldeoxybenzoins were prepared by reported procedures[27] and were purified by column chromatography (silica gel/hexane). Spectral data for analytically pure materials were reported by us earlier.[17]

Zeolites 13X (NaX) and LZ-Y52 (NaY) were obtained from Linde. The cation of interest was exchanged into these powders by contacting the material with the appropriate nitrate solution at 90 °C. For each gram of zeolite, 10 mL of a 10% nitrate solution was used. This was repeated a number of times. The samples were then thoroughly washed with water and dried. Exchange loadings were typically between 37 and 84%. Exchange levels for individual zeolites were as follows: LiX, 46%; KX, 64%; RbX, 49%; CsX, 37%; LiY, 64%; KY, 84%; RbY, 68%; CsY, 62%. Prior to use these samples were heated in a furnace at 500 °C in air for about 10 h. Activated zeolites were used immediately.

Inclusion of Ketones within Zeolites. Known amounts of benzoin ethers/alkyldeoxybenzoins and the activated zeolites were stirred together in 20 mL of hexane for about 10 h. In a typical preparation 250 mg of the zeolite and 5 mg of the ketone were taken in 20 mL of the solvent. White powder collected by filtration of the solvent was washed with ether twice and dried under nitrogen. Samples were taken in Pyrex cells fitted with Teflon-brand stopcocks, degassed thoroughly (10^{-4} mm), and sealed. These samples were generally dry and contained less than 1% of water.

Photolysis and Isolation of Products. Samples containing 125 mg of the complex were degassed in Pyrex cells and irradiated with 450-W mercury lamps. Irradiation cells were rotated periodically to provide uniform exposure. Generally about 15% conversion was obtained in about 2 h of irradiation. After photolysis products were extracted by stirring the samples in ether (20 mL) for about 6 h. In some cases the zeolite was dissolved with concentrated HCl and extracted with ether. Control experiments established that the products are stable to the acid extraction conditions. Products were analyzed by GC (Hewlett Packard Model 5890; SE-30 capillary column), using *trans*-stilbene as the internal standard. Structures of all products have been established earlier and the spectral data are consistent with the literature reports.[17]

Acknowledgment. We thank A. Pittman and P. Hollins for valuable technical assistance and N. J. Turro for useful discussions.

(27) Fisher, E. *Chem. Ber.* **1893**, *26*, 2412.

Synthetic and Kinetic Studies of the Intramolecular Diels-Alder Reactions of Cycloalkenylallenylphosphine Oxides

Michael L. Curtin and William H. Okamura*

Department of Chemistry, University of California, Riverside, California 92521

Received March 28, 1990

Kinetic investigations reveal that diphenylphosphinoyl (diphenylphosphine oxide) substituted cycloalkenylallenes **13b-d** undergo intramolecular Diels-Alder (IMDA) cyclizations at room temperature to afford adducts with *gem*-dialkyl effect accelerations of 4.6 (*gem*-dimethyl), 21.1 (*gem*-diethyl), and 27.8 (*gem*-dipropyl), respectively, relative to **13a**. Arrhenius data reveals $\Delta G^{\ddagger}$'s of between 22.1 and 23.9 kcal/mol for vinylallenes **13a-c**. Vinylallenes **24** and **25** revealed mono-*tert*-butyl acceleration effects of 70.5 and 205, respectively, relative to the parent **13a**. Cycloalkenyl ring size studies showed that vinylallenes **13b** and **33a-c** had cyclization rates within a factor of 10 of one another. Tether length studies revealed that the three carbon tethered allene **43b** exhibits an 850-fold decrease in cyclization rate versus the two carbon tethered allene **13b**. A comparison of the rate of IMDA cyclization of the three carbon tethered **43a** and **43b** revealed a *gem*-dimethyl effect of 2.6, quite similar in magnitude to the 4.6 value observed for the two carbon tethered derivatives **13a** and **13b**. An X-ray crystallographic analysis of **34a** firmly established the stereochemical course of the reaction, including the anti relationship of the bridgehead hydrogens in the resulting polycycles.

Introduction

For the vinylallenic variant of the intramolecular Diels-Alder (IMDA) reaction[1-3] in which the vinylallene serves as the diene component of the reaction, there are five ways in which diene and dienophile can be tethered (Chart I).[1,4,5] As depicted in Scheme I, because of the rigidity of vinylallenyl system 1, the type I IMDA cyclization was anticipated to lead to polycycle **2** in a completely regio-, enantio-, and diastereoselective manner. Indeed, the complete facial selectivity of this reaction was

(1) Okamura, W. H.; Curtin, M. L. *Synlett* **1990**, 1.

(2) For reviews of the chemistry of vinylallenes, see: (a) Egenburg, I. Z. *Russ. Chem. Rev.* **1978**, *47*, 470. (b) Okamura, W. H. *Acc. Chem. Res.* **1983**, *16*, 81.

(3) For reviews of the IMDA reaction, see: (a) Craig, D. *Chem. Soc. Rev.* **1987**, *16*, 187. (b) Fallis, A. G. *Can. J. Chem.* **1984**, *62*, 183. (c) Ciganek, E. *Org. React.* **1984**, *32*, 1.

(4) Type I IMDA reactions: (a) Deutsch, E. A.; Snider, B. B. *J. Org. Chem.* **1982**, *47*, 2682. (b) Deutsch, E. A.; Snider, B. B. *Tetrahedron Lett.* **1983**, *24*, 3701. (c) Snider, B. B.; Burbaum, B. W. *J. Org. Chem.* **1983**, *48*, 4370. (d) Keck, G. E.; Kachensky, D. F. *J. Org. Chem.* **1986**, *51*, 2487.

(5) Type V_E IMDA reactions: (a) Reich, H. J.; Eisenhart, E. K. *J. Org. Chem.* **1984**, *49*, 5282. (b) Reich, H. J.; Eisenhart, E. K.; Olson, R. E.; Kelly, M. J. *J. Am. Chem. Soc.* **1986**, *108*, 7791.

0022-3263/90/1955-5278$02.50/0